

Dynamic recrystallization of quartz: correlation between natural and experimental conditions

MICHAEL STIPP, HOLGER STÜNITZ, RENÉE HEILBRONNER
& STEFAN M. SCHMID

*Department of Earth Sciences, Basel University, Bernoullistrasse 32, 4056 Basel, Switzerland
(e-mail: Michael.Stipp@unibas.ch)*

Abstract: Quartz veins in the Eastern Tonale mylonite zone (Italian Alps) were deformed in strike-slip shear. Due to the synkinematic emplacement of the Adamello Pluton, a temperature gradient between 280 °C and 700 °C was effected across this fault zone. The resulting dynamic recrystallization microstructures are characteristic of bulging recrystallization, subgrain rotation recrystallization and grain boundary migration recrystallization. The transitions in recrystallization mechanisms are marked by discrete changes of grain size dependence on temperature. Differential stresses are calculated from the recrystallized grain size data using paleopiezometric relationships. Deformation temperatures are obtained from metamorphic reactions in the deformed host rock. Flow stresses and deformation temperatures are used to determine the strain rate of the Tonale mylonites through integration with several published flow laws yielding an average rate of approximately 10^{-14} s $^{-1}$ to 10^{-12} s $^{-1}$. The deformation conditions of the natural fault rocks are compared and correlated with three experimental dislocation creep regimes of quartz of Hirth & Tullis. Linking the microstructures of the naturally and experimentally deformed quartz rocks, a recrystallization mechanism map is presented. This map permits the derivation of temperature and strain rate for mylonitic fault rocks once the recrystallization mechanism is known.

Introduction

Dynamic recrystallization is in many materials primarily the result of two processes: (1) the formation and progressive rotation of subgrains; and (2) grain boundary migration (e.g. Guillopé & Poirier 1979; Urai *et al.* 1986). The interaction of these two processes is responsible for the occurrence of three different mechanisms of dynamic recrystallization forming characteristic microstructures. These are termed bulging recrystallization (BLG; e.g. Bailey & Hirsch 1962; Drury *et al.* 1985), subgrain rotation recrystallization (SGR; e.g. Hobbs 1968; White 1973; Guillopé & Poirier 1979) and grain boundary migration recrystallization (GBM; e.g. Guillopé & Poirier 1979; Means 1983; Urai *et al.* 1986; Jessell 1987). We observe similar recrystallization microstructures in quartz as have been described for other materials; thus we infer that the recrystallization mechanisms vary with temperature in the same way as they do in those materials (cf. Stipp *et al.* 2002). During BLG at low temperature conditions, local grain boundary migration is the dominant process. The contribution of subgrain rotation increases with temperature, until subgrain rotation dominates the recrystallization, and the resulting microstructures are those of SGR. At still higher temperatures above the range of SGR, the dominant recrystallization mechanism

is GBM (cf. Guillopé & Poirier 1979; Urai *et al.* 1986). The dominant recrystallization process is again grain boundary migration, but boundaries sweep entire grains, so that in many cases there is no reduction in grain size.

In an experimental study, Hirth & Tullis (1992) have identified three dislocation creep regimes for quartz. The definition of the dislocation creep regimes is based on mechanical data and on recrystallization mechanisms identified by TEM and light microscope observations. Hirth & Tullis (1992) have demonstrated that the dominant recrystallization mechanism is controlled by temperature, stress and strain rate. The delineation of the different microstructural regimes reflects the relative rates of grain boundary migration, dislocation climb and dislocation production. In regime 1, recovery and recrystallization are mainly accommodated by strain-induced grain boundary migration, in regime 2 by climb-controlled dislocation creep (subgrain rotation) and in regime 3 by both grain boundary migration and subgrain rotation (Hirth & Tullis 1992). In a number of studies, the experimentally produced microstructures have been correlated with dynamic recrystallization microstructures of naturally deformed rocks (Dunlap *et al.* 1997; Snoke *et al.* 1998; Stöckhert *et al.* 1999; Hirth *et al.* 2001; Zulauf 2001). However, due to the given geological settings and outcrop conditions, none of these studies included

the full range of dynamic recrystallization microstructures of quartz occurring in natural fault rocks. Some microstructural transitions were missing and the field samples were derived from different shear zones, so that the deformation conditions may have varied significantly.

The Eastern Tonale fault zone exposes a set of outcrops where the whole range of natural dynamic recrystallization microstructures of quartz can be observed within a single shear zone (Stipp *et al.* 2002). Deformation temperatures ranging from approximately 280 °C to 700 °C were derived from synkinematic mineral assemblages. The recrystallized grain sizes were measured in samples of different deformation temperatures. In this contribution, differential stresses have been inferred from paleopiezometry, and strain rates have been inferred from published flow laws of quartz. Combining the data of these naturally deformed rocks with the experimental data of Hirth & Tullis (1992), a recrystallization mechanism map will be constructed. Such a map, in conjunction with careful microstructural observations, will help geologists to determine or constrain the deformation conditions in quartz-rich mylonites from natural shear zones.

Geological setting

The Eastern Tonale Line in the Italian Alps is a dextral strike-slip segment of the Periadriatic fault system. In the area of interest, the fault zone was heated by the synkinematic Oligocene emplacement of the Presanella intrusion of the Adamello pluton (Fig. 1). The contact aureole of the pluton extends across the fault zone, which is 800 m wide and exhibits a vertical mylonitic foliation and a subhorizontal stretching lineation. Farther west, the Tonale Line is deformed entirely by brittle deformation (Werling 1992; Stipp & Schmid 1998). At the eastern border of the Adamello pluton, the Tonale Line is cut by the sinistral Giudicarie strike-slip zone. Near the pluton, the strike-slip fault includes the mylonitic rim of the Presanella intrusion in the south, followed by the Tonale mylonites of the Southern Mylonite Zone and the cataclasites towards the north (Fig. 1). The Stavel mylonites of the Northern Mylonite

Zone (Fig. 1) situated north of the cataclasites are not part of this study as they belong to an older deformation stage (Werling 1992).

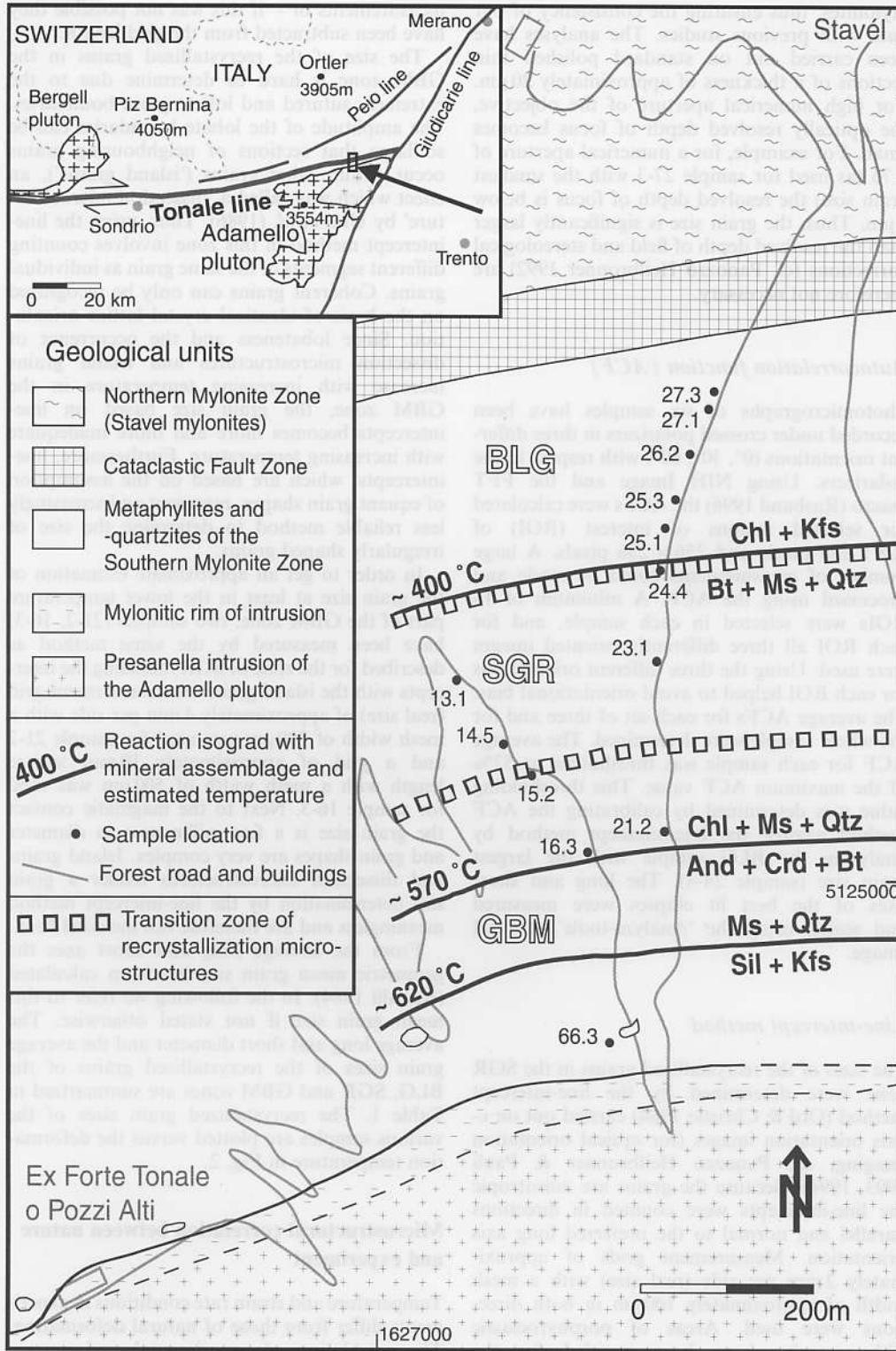
From north to south there is a temperature gradient ranging from 250 °C to about 700 °C in the Tonale mylonites (Fig. 1) at a constant confining pressure of 250 to 300 MPa. These P–T estimates are based on critical mineral assemblages and related reaction isograds in the metasediments of the Tonale mylonites (Werling 1992; Stipp *et al.* 2002). Quartz microstructures show that the transition from dominantly brittle to dominantly crystal plastic deformation occurs at about 280 °C. Three microstructural zones have been recognized corresponding to the three different dynamic recrystallization mechanisms of quartz (Fig. 1). Bulging recrystallization (zone of BLG) dominates from approximately 280–400 °C, subgrain rotation recrystallization (zone of SGR) from approximately 400–500 °C and grain boundary migration recrystallization (zone of GBM) from approximately 500 °C to about 700 °C at the magmatic contact (Stipp *et al.* 2002).

Quartz veins taken from the Southern Mylonite Zone were used for the microstructural analysis (Fig. 1) because they contain fewer inclusions than quartzites or quartz layers in polymineralic mylonites. Only foliation-parallel veins were sampled and it was ensured that the dynamic recrystallization microstructures in the veins were the same as those in quartz within the metasedimentary host rocks.

Determination of recrystallized grain size

The mylonitic quartz veins have been analysed in X–Z sections, i.e. normal to the foliation and parallel to the stretching lineation. The microstructural characterization and the grain size analyses have been carried out using image analysis methods. In the zone of BLG, grain sizes have been determined using the autocorrelation function (ACF; Panozzo Heilbronner 1992). In the zones of SGR and GBM, the line-intercept method (Smith & Guttman 1953, cited in Ord & Christie 1984) was used. This method was chosen because it has been used for most of the experimentally calibrated piezometers as well as for previous studies on natural quartz

Fig. 1. Map of investigated area of the Tonale fault zone; temperatures and reaction isograds are inferred from mineral assemblages of metasediments (data from Werling 1992 and Stipp *et al.* 2002). Three zones of dynamic recrystallization microstructures are distinguished: BLG (bulging recrystallization); SGR (subgrain rotation recrystallization); and GBM (grain boundary migration recrystallization). Geographical coordinates refer to sheet 'Passo del Tonale' of the autonomous province of Trento (Italy; Carta Topografica Generale No. 041120, 1987). Inset: Regional setting of the investigated area (arrow).



mylonites, thus ensuring the consistency of our data with previous studies. The analyses have been carried out on standard polished thin sections of a thickness of approximately 20 μm . For high numerical aperture of the objective, the optically resolved depth of focus becomes small. For example, for a numerical aperture of 0.75 (as used for sample 27-3 with the smallest grain size) the resolved depth of focus is below 1 μm . Thus, the grain size is significantly larger than the resolved depth of field and stereological corrections (cf. Panozzo Heilbronner 1992) are therefore not necessary.

Autocorrelation function (ACF)

Photomicrographs of six samples have been recorded under crossed polarizers in three different orientations (0° , 30° , 60°) with respect to the polarizers. Using NIH Image and the FFT macro (Rasband 1996) the ACFs were calculated for selected regions of interest (ROI) of 128×128 pixels and 256×256 pixels. A large number of measurements could be made and processed using the ACF. A minimum of 16 ROIs were selected in each sample, and for each ROI all three differently oriented images were used. Using the three different orientations for each ROI helped to avoid orientational bias. The average ACFs for each set of three and for the whole sample were determined. The average ACF for each sample was thresholded at 52% of the maximum ACF value. This thresholding value was determined by calibrating the ACF method against the line-intercept method by analysing the BLG sample with the largest grain size (sample 24-4). The long and short axes of the best fit ellipses were measured and scaled using the 'Analyze-tools' of NIH Image.

Line-intercept method

The sizes of the recrystallized grains in the SGR zone were determined by the line-intercept method (Ord & Christie 1984) carried out on *c*-axis orientation images (for optical orientation imaging, see Panozzo Heilbronner & Pauli 1993, 1994). Because the grains are anisotropic the line-intercepts were counted in directions parallel and normal to the preferred long axis orientation. Measurement grids of approximately 2 mm per side (real size) with a mesh width of approximately 100 μm in both directions were used. Areas of porphyroclastic ribbon grains have been avoided for the

measurements or – if this was not possible they have been subtracted from the grid length.

The size of the recrystallized grains in the GBM zone is hard to determine due to the extremely sutured and lobate grain boundaries. The amplitude of the lobate boundaries can be so large that sections of neighbouring grains occur within other grains ('island grains'), an effect which was called a 'dissection microstructure' by Urai *et al.* (1986). Thus, using the line-intercept method in this zone involves counting different segments of the same grain as individual grains. Coherent grains can only be recognized on the basis of identical crystal lattice orientation. Since lobateness and the occurrence of dissection microstructures and island grains increase with increasing temperature in the GBM zone, the grain size based on line-intercepts becomes more and more inadequate with increasing temperature. Furthermore, line-intercepts, which are based on the assumption of equant grain shapes, represent an increasingly less reliable method to determine the size of irregularly shaped grains.

In order to get an approximate estimation of the grain size at least in the lower temperature part of the GBM zone, two samples (21-2, 16-3) have been measured by the same method as described for the zone of SGR including the intercepts with the island grains. A measurement grid (real size) of approximately 4 mm per side with a mesh width of 200 μm was used for sample 21-2 and a grid of approximately 10 mm square length with a mesh width of 500 μm was used for sample 16-3. Next to the magmatic contact the grain size is a few millimetres in diameter and grain shapes are very complex. Island grains and dissection microstructures render a grain size determination by the line-intercept method meaningless and are therefore not included here.

From the average long and short axes the geometric mean grain size has been calculated (Ranalli 1984). In the following we refer to this mean grain size if not stated otherwise. The average long and short diameter and the average grain sizes of the recrystallized grains of the BLG, SGR and GBM zones are summarized in Table 1. The recrystallized grain sizes of the various samples are plotted versus the deformation temperature in Fig. 2.

Microstructural correlation between nature and experiment

Temperature and strain rate conditions in experiments differ from those of natural deformation. The correlation of experimental and natural

Table 1. Recrystallized grain sizes

Sample	Longitudinal coordinate	Latitudinal coordinate	Long axis [μm]	Short axis [μm]	Mean grain size [μm]
<i>BLG</i>					
27-3	1627425	5125605	6.2	4.9	5.5
27-1	1627415	5125595	9.3	6.6	7.8
26-2	1627395	5125555	9.9	7.6	8.7
25-3	1627375	5125500	17.1	11.9	14.3
25-1	1627365	5125475	25.1	9.5	15.5
24-4	1627355	5125440	28.6	20.6	24.3
<i>SGR</i>					
13-1	1627090	5125220	78	43	58
23-1	1627330	5125345	89	42	61
14-5	1627140	5125155	113	49	74
15-2	1627185	5125125	134	53	84
<i>GBM</i>					
21-2	1627320	5125190	289	166	219
16-3	1627250	5125040	440	285	354

Recrystallized grain sizes of the investigated samples taken from different zones of dynamic recrystallization. Mean grain size is the geometric mean of grain long and short axes. For method of grain size measurement see text. Geographical coordinates refer to sheet 'Passo del Tonale' of the autonomous province of Trento (Italy; Carta Topografica Generale No. 041120, 1987).

deformation depends upon the operation of the same deformation mechanisms, which should produce identical microstructures at strain-independent steady state flow stress conditions. Transitions from one recrystallization mechanism to another cause microstructural changes which can be observed in both nature and experiments. We therefore focus on microstructures

when relating nature to experiments. A reliable correlation of microstructures rests on clearly identifiable microstructural criteria. Of particular interest are distinctly different microstructures because they indicate switches in the dominant dynamic recrystallization mechanisms. Mercier (1980), Hirth & Tullis (1992) and Zulauf (2001) reported a step in the grain size-temperature relationship as the most obvious microstructural discontinuity. Our data indicate that this discontinuity is not a step, but rather a discrete change in the slope of the grain size-temperature relationship.

In the Tonale mylonites, there are two slope changes (Fig. 2) which coincide with transitions in the dominant dynamic recrystallization mechanism. Other microstructural criteria, e.g. shape and lobateness, change more slowly or gradually so that they can only be used in combination to define transitions in the dominant recrystallization mechanism. As a first approximation the three dislocation creep regimes defined by Hirth & Tullis (1992) can be correlated with the three dominant dynamic recrystallization mechanisms inferred from the deformed Tonale quartz veins (Stipp *et al.* 2002). However, the transitions from BLG to SGR and from SGR to GBM do not coincide with the transitions from regime 1 to regime 2 and from regime 2 to regime 3, respectively. In the following we will describe the microstructural transitions which are the basis for our correlation of the dynamic recrystallization mechanisms in the Tonale

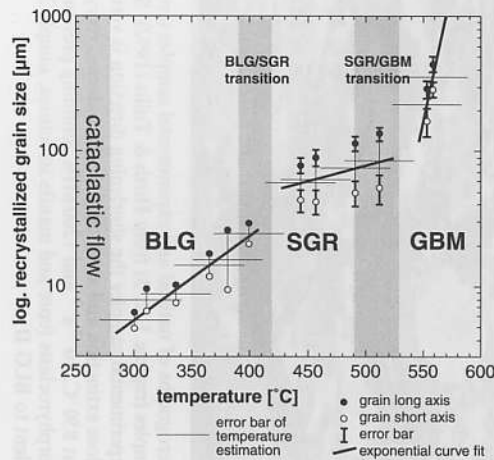


Fig. 2. Plot of recrystallized grain size versus deformation temperature; long and short axes of recrystallized grains and best fits of geometric mean grain size are shown. Error bars are one standard deviation; for technical reasons there are no error bars for the BLG data.

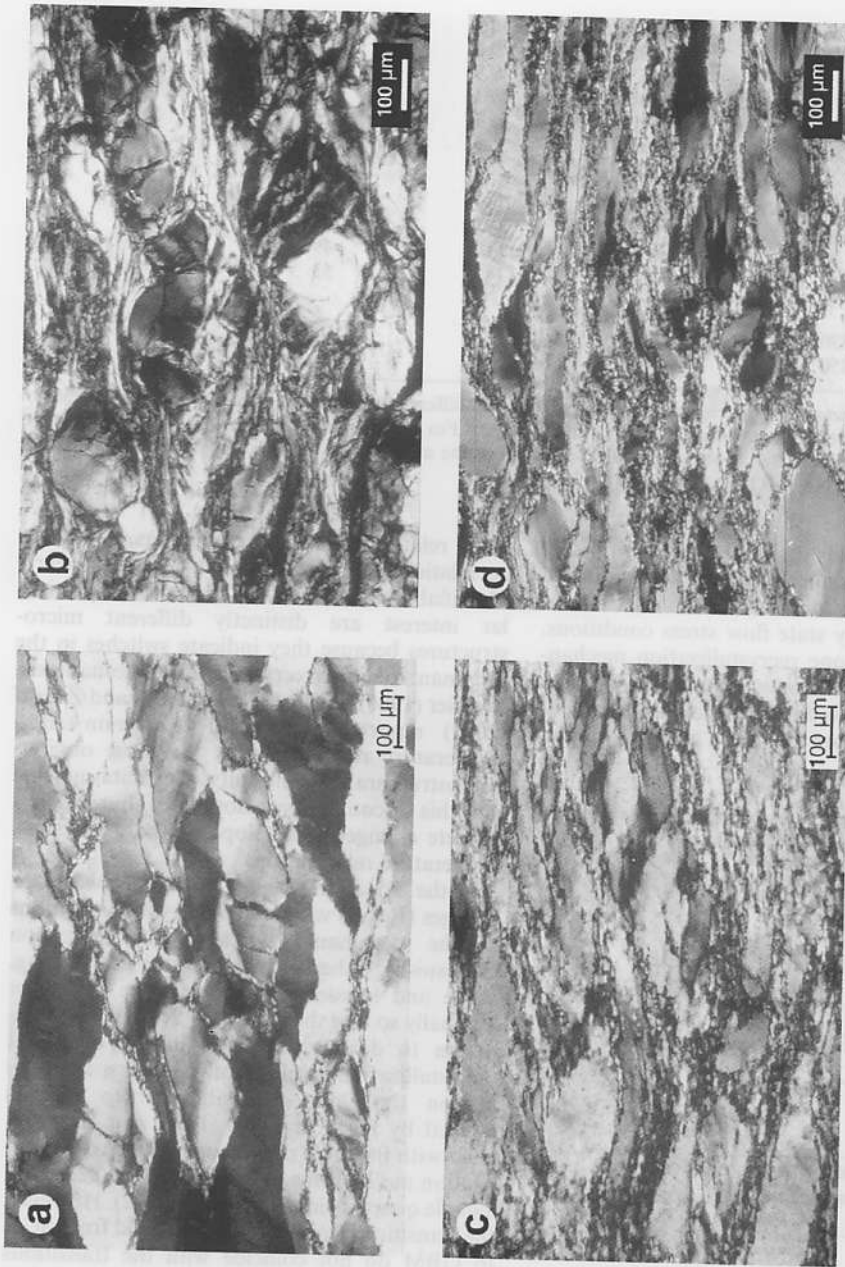


Fig. 3. Light micrographs of natural and experimental samples (crossed polarizers). Mylonitic quartz veins from the Eastern Tonale line (BLG, SGR, GBM) and experimental samples (regime 1, 2, 3) from Hirth & Tullis (1992). Samples are oriented normal to the main foliation. In natural samples the stretching lineation is horizontal. In experimental samples the shortening direction is vertical (micrographs taken from Tullis *et al.* 2000). (a) BLG I (c. 310 °C): Quartz porphyroclasts displaying undulose extinction and serrated grain boundaries and fractures (sample 27-1). (b) Regime 1: Heavily recrystallized quartzite shortened 65% at 850 °C, 10^{-5} s $^{-1}$ and 1200 MPa confining pressure (equivalent to BLG I). (c) BLG II (c. 370 °C): Recrystallization preferentially along serrated grain boundaries of porphyroclasts (core and mantle structures, sample 25-3). (d) Regime 2: Heavily recrystallized quartzite shortened 64% at 800 °C, 10^{-6} s $^{-1}$ and 1200 MPa confining pressure (equivalent to BLG II).

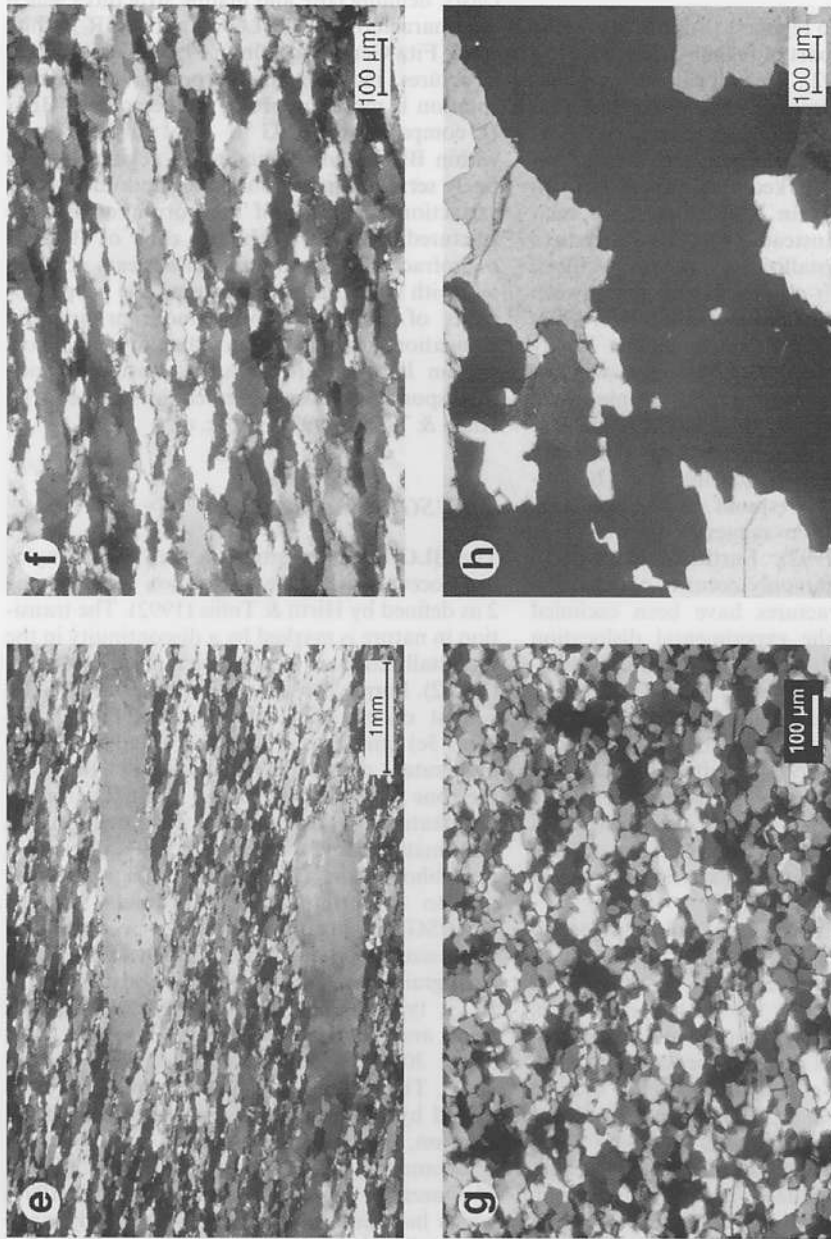


Fig. 3. (e) SGR (*c.* 510 °C): Polygonization and recrystallization of ribbon grains at the SGR/GBM-transition; recrystallized grains and subgrains have nearly the same grain sizes and shapes (sample 15-2; note the different scale). (f) SGR (*c.* 510 °C): Detail of (e) showing recrystallized grains only; recrystallized grains display sutured and weakly lobate grain boundaries indicating a contribution of grain boundary migration close to the SGR/GBM-transition (sample 15-2). (g) Regime 3: Black Hills quartzite shortened 50% at 1200 °C, 10^{-6} s $^{-1}$ and 1200 MPa confining pressure. (h) GBM II (*c.* 650 °C): Amoeboid grain shapes, islands grains, very large recrystallized grain sizes (sample 66-3).

mylonites with the experimentally derived dislocation creep regimes of Hirth & Tullis (1992).

Variation within the zone of BLG

BLG corresponds to regime 1 (Fig. 3a, b) and the lower temperature part of regime 2 (Fig. 3c, d) of Hirth & Tullis (1992). We will call the part that corresponds to regime 1, BLG I, and the part that corresponds to the lower temperature part of regime 2, BLG II. The transition from BLG I to BLG II is not marked by a discontinuity in the recrystallized grain size–temperature relationship (Fig. 2). Instead, there are differences in dynamic recrystallization microstructures, which allow us to define a change between BLG I and BLG II. Hirth & Tullis (1992, 1994) attribute the recrystallization in regime 1 only to grain boundary migration processes without subgrain rotation. In the natural samples from the Eastern Tonale fault zone, BLG I porphyroclasts show (in the light microscope) some very small subgrains along the serrated grain boundaries which may correspond to the cell misorientation mechanism suggested for regime 1 (Hirth & Tullis 1992). Furthermore, BLG I microstructures commonly occur in conjunction with fractures. Fractures have been excluded for regime 1 of the experimental dislocation creep regimes and attributed to the brittle–plastic transition (Hirth & Tullis 1994). In nature, however, the confining pressure can be low at the brittle–plastic or frictional–viscous (Schmid & Handy 1991) transition. When local differential stresses reach the magnitude of the effective confining pressure, fracturing can occur in alternation with dynamic recrystallization in natural mylonites (cf. coseismic creep of Küster & Stöckhert 1999).

Microfracturing and related solution-deposition (cf. Hippert & Egydio-Silva 1996) can be neglected for the formation of new grains in the Tonale mylonites. We think that in nature, apart from subgrain rotation, microfracturing is another important potential process for separating bulges from porphyroclasts (van Daalen *et al.* 1999; Stipp *et al.* 2002). Fracture zones are bulged, and bulges and new grains along these fractures have the same size as bulges, subgrains and recrystallized grains along grain boundaries. The increasing amount and size of recrystallized grains with increasing temperature within the zone of BLG occurs together with a change in the preferred sites of dynamic recrystallization between BLG I and BLG II. In BLG I, recrystallization occurs preferentially at triple junctions of porphyroclasts (cf. Stipp *et al.*

2002), whereas the porphyroclasts in BLG II are completely surrounded by recrystallized grains (Fig. 3c, d). Subgrains of the same size as the bulges are detectable in the light microscope near the grain boundary region of the porphyroclasts, defining core and mantle structures which are characteristic of BLG II and SGR (White 1976; Fitz Gerald & Stünitz 1993). These microstructures indicate that progressive subgrain rotation is more important in the zone of BLG II compared to BLG I. The porphyroclasts within BLG I corresponding to regime 1 show finely serrated grain boundaries and undulatory extinction and some of the porphyroclasts are fractured (Fig. 3a, b). In the zone of BLG II microfracturing is rare and disappears completely with increasing temperature. The porphyroclasts of BLG II show a more pronounced elongation, and undulatory extinction and deformation lamellae are frequent, features, which correspond to those observed in regime 2 by Hirth & Tullis (1992; Fig. 3c, d).

BLG/SGR-transition

The BLG/SGR transition in the Tonale mylonites occurs within the dislocation creep regime 2 as defined by Hirth & Tullis (1992). The transition in nature is marked by a discontinuity in the recrystallized grain size–temperature relationship (Fig. 2). Porphyroclasts within the zone of SGR consist of extremely elongated ribbon grains (Fig. 3e) contrasting with the angular or only moderately elongated porphyroclasts found in the zone of BLG (Fig. 3a–d). Internal deformation features such as undulatory extinction and deformation lamellae occur occasionally within the ribbon grains (Fig. 3e); they may partly be due to overprinting during cooling. At the BLG/SGR transition, both the recrystallized grain size and the volume fraction of recrystallized grains increase significantly. In the zone of BLG, typically less than 20% of the quartz veins are recrystallized. In the zone of SGR about 30–80% are recrystallized (Stipp *et al.* 2002). The ribbon grains are progressively consumed by polygonization (progressive subgrain rotation, Fig. 3e).

Geometric dynamic recrystallization (GRX; McQueen *et al.* 1985; Doherty *et al.* 1997) which has been described as a type of dynamic recrystallization which occurs in metals at high deformation temperature and large strain can produce microstructures similar to those referred to as BLG II and SGR (Fig. 3c–g). If GRX occurs at low deformation temperature, as pointed out by Humphreys & Hatherly (1996),

it cannot be distinguished from continuous recrystallization phenomena, i.e. subgrain rotation recrystallization. Hence, the application of the term GRX to the investigated quartz samples might be possible, but would not change the microstructural correlation, because microstructures similar to GRX also occur in the experimental sample set of Hirth & Tullis (1992; cf. Fig. 3).

SGR/GBM-transition

The SGR/GBM transition in nature (Fig. 3f) falls within regime 3 of the experimental dislocation creep regimes (Fig. 3g). Microstructures typical for GBM in nature are not attainable experimentally due to the onset of melting. Within the natural samples, this transition is again marked by a discontinuity in the recrystallized grain size-temperature relationship (Fig. 2). Recrystallized grains of the GBM zone show irregular grain shapes and a broad grain size distribution within a single sample. In contrast, the recrystallized grains of the SGR zone have rather constant grain shapes and sizes, which are almost identical to those of the subgrains observed in the light microscope. At the transition to GBM, the recrystallized grain size is somewhat larger than the subgrain size as visible in the light microscope. The recrystallized grain size distribution in the zone of GBM is broader and the grains display weakly sutured grain boundaries (Fig. 3e,f). GBM-microstructures (Fig. 3h) differ from regime 3 (Fig. 3g) in that they show larger grain sizes and more irregular grain shapes with more sutured grain boundaries and amoeboid grain shapes. Dissection microstructures (Urai *et al.* 1986) and 2D-island grains, which are typical for GBM (Fig. 3h), have not been found in regime 3 of Hirth & Tullis (1992). Instead, in regime 3 (Fig. 3g) grains are of similar size and shape, and grain sizes are comparable or even smaller than those of the uppermost SGR (compare grain sizes in Fig. 3f,g). Natural samples of the GBM zone are completely recrystallized. The transition to completely recrystallized microstructures occurs in the experiments of Hirth & Tullis (1992) and in the samples of the Tonale mylonites at the SGR/GBM transition.

The zone of GBM of the Tonale mylonites can be divided into a lower and a higher temperature part, GBM I and GBM II, respectively (Stipp *et al.* 2002). However, GBM II samples were not considered in this study because: (1) these microstructures are not attainable experimentally; and (2) due to the lobateness of grain

boundaries, it is very difficult to determine grain sizes in such microstructures, as pointed out above.

Stress and strain rate calculations

The correlation of the experimental dislocation creep regimes and the natural zones of dynamic recrystallization is summarized in a schematic diagram (Fig. 4). In experiments, the same microstructural transitions take place at higher temperatures and at strain rates that are 5 to 10 orders of magnitude higher than in nature (e.g. Hobbs *et al.* 1976; Mercier *et al.* 1977; Suppe 1985; Twiss & Moores 1992). Assuming that the rheological properties are conformable in nature and experiment, a strain rate/temperature extrapolation can be made (cf. Paterson 1987). Through a stress determination (paleopiezometry) and using flow law equations (deformation temperature is known), the strain rate in the natural mylonites can be calculated.

Paleopiezometry

The paleostress, which is inferred to be the steady-state flow stress at the time of deformation, can be determined by different microstructural paleopiezometers. These are either based on the density of unbound dislocations (e.g. Weertman 1970; Goetze & Kohlstedt 1973; Takeuchi & Argon 1976), on the subgrain size (e.g. Raleigh & Kirby 1970; Twiss 1986), or on the recrystallized grain size (e.g. Luton & Sellars 1969; Mercier *et al.* 1977; Twiss 1977). Although only the first two types of piezometers are based on physical models, we have used a recrystallized grain size piezometer which is largely empirical. Both the subgrain size and the dislocation density are much more sensitive to annealing and retrograde overprinting and thus the recrystallized grain size has been characterized as the feature with the highest inherent stability in naturally deformed rocks (Mercier *et al.* 1977; White 1979; Kohlstedt & Weathers 1980). Recrystallized grain size piezometers have been calibrated in the form

$$\Delta\sigma = BD^{-x}, \quad (1)$$

where $\Delta\sigma$ is the steady state differential stress, D is the recrystallized grain size and B and x are empirical constants. More recently, several microphysical models have been proposed to explain the piezometric relationship (Edward *et al.* 1982 for subgrain size; Derby & Ashby 1987; Derby 1990; Shimizu 1998; de Bresser

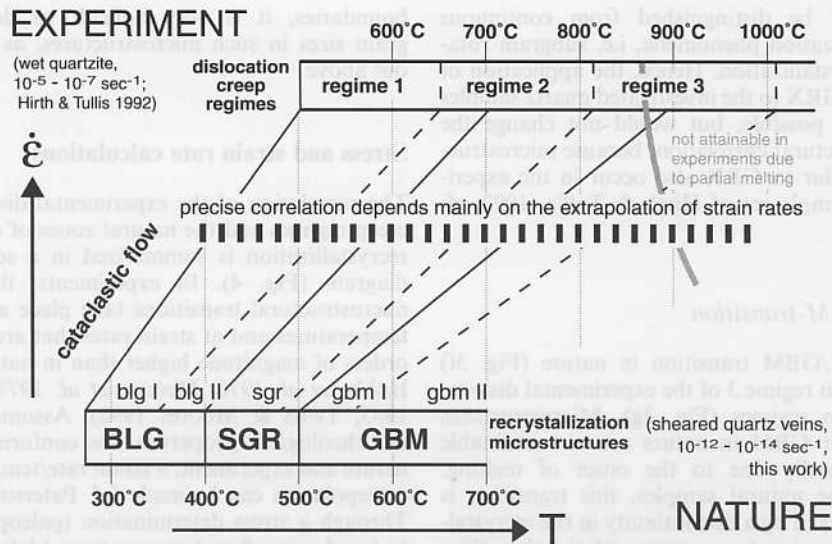


Fig. 4. Schematic diagram illustrating the ranges of temperature and strain rate of the natural zones of dynamic recrystallization and of the experimental dislocation creep regimes of Hirth & Tullis (1992). At slow strain rates, three main types of microstructures can be distinguished: bulging recrystallization (BLG); subgrain rotation recrystallization (SGR); and grain boundary migration recrystallization (GBM). Subdivisions of these main recrystallization microstructures can be correlated with the experimental dislocation creep regimes. Solid lines mark the transitions between BLG, SGR and GBM and their corresponding experimental microstructures; dashed lines mark the transitions in experimental dislocation creep regimes and their corresponding microstructures in nature.

et al. 1998 for recrystallized grain size). Since all these theoretical models have not yet been calibrated and used for dynamic recrystallization of quartz in natural fault rocks, we chose not to use piezometric relationships corresponding to these models. However, a recent review on piezometric relationships (de Bresser *et al.* 2001) emphasizes the need to test and calibrate theoretical models with new experimental studies. When such studies are available they can be used to critically evaluate and expand the considerations made below.

For any given grain size the piezometers for quartz (Mercier *et al.* 1977; Twiss 1977, 1980; Christie *et al.* 1980; Koch 1983 and Mainprice 1981 in Koch 1983) yield a stress range for the dynamically recrystallized grain sizes of more than one order of magnitude (Fig. 5). Wet quartzite conditions are much more realistic for the deformation in natural mylonitic shear zones and we therefore consider only piezometers calibrated for 'wet' conditions and the one which is based on the theoretical assumptions of Twiss (1977, 1980) for Fig. 6. The data of Mercier *et al.* (1977) and Mainprice (1981) are not reliable with respect to the water content of the samples. Furthermore, either the experimental constraints on the mechanical data are poor (solid confining medium for the experiments

used in Mercier *et al.* 1977), or the choice of the starting material is not very satisfying (Dover flint in Mainprice 1981), because the finite deformation microstructures differ significantly from those found in natural quartz mylonites. Therefore, these calibrations have not been included in Fig. 6.

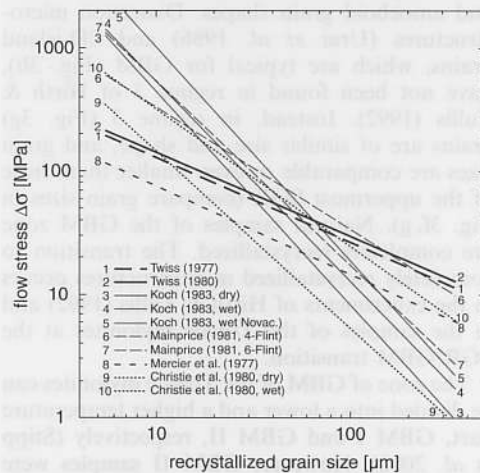


Fig. 5. Diagram of recrystallized grain size paleopiezometers of quartz; the piezometers of Mainprice (1981) were calculated by Koch (1983).

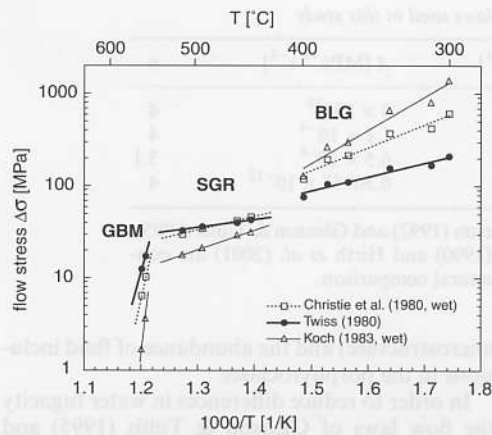


Fig. 6. Flow stresses calculated from recrystallized grain sizes using different piezometers. Empirical constants B , x are 4090, 1.11 for the piezometer of Christie *et al.* (1980), 676, 0.68 for Twiss (1980) and 21829, 1.61 for Koch (1983). The slopes of the best fits vary for each of the recrystallization mechanisms.

The wet piezometers of Christie *et al.* (1980) and Koch (1983) yield unrealistically high values for stress at the small grain sizes of BLG. This can probably be related to the poor experimental constraints on the mechanical data (see Gleason & Tullis 1993, 1995 for discussion). For sample 27-3, which has been deformed under the lowest temperature conditions, the flow stresses predicted by the different paleopiezometers in Fig. 6 range from 212 MPa (Twiss 1980) to 1396 MPa (Koch 1983, wet). The piezometers of Koch (1983) and Christie *et al.* (1980) predict differential stresses for BLG which are much higher than the confining pressure (250 to 300 MPa) derived from coexisting mineral assemblages (Stipp *et al.* 2002). Such high stresses would produce dominant brittle deformation (Hirth & Tullis 1994; Kohlstedt *et al.* 1995) instead of low temperature crystal plasticity. Dominantly brittle deformation microstructures have not been observed. Hence, the piezometers of Christie (1980, wet) and Koch (1983, wet) can be excluded.

For the entire sample set, including BLG I through GBM I, the piezometer of Twiss (1980) yields stresses from 212 MPa to 12.5 MPa (Fig. 6). The extrapolation of this flow stress range to the brittle-plastic transition, corresponding to the transition from the Cataclastic Fault Zone to the Southern Mylonite Zone of the Tonale Line at 280 °C (Fig. 1), yields a differential stress of about 250 MPa (Fig. 6). The confining pressure of 250 to 300 MPa derived from critical mineral assemblages is approximately

equal to this differential stress magnitude at the brittle-plastic transition. Empirically, the high confining pressure limit of semibrittle deformation is reached when confining pressure and differential stress are of approximately the same magnitude (Kirby 1980; Evans *et al.* 1990; Kohlstedt *et al.* 1995). Thus the paleopiezometer of Twiss (1980) and our microstructural observations yield consistent results for the brittle-plastic transition. Paleopiezometers appropriate for the individual different recrystallization mechanisms are not calibrated for quartz as has been found experimentally for other minerals (see evaluation of paleopiezometers). The paleopiezometer by Twiss (1977, 1980) appears to be the most suitable calibration for our samples in the light of the geological constraints for the data and therefore it has been used in this study (cf. Gleason & Tullis 1993, 1995).

Strain rate estimation

The strain rate is related to flow stress and temperature by experimentally derived flow laws (e.g. Heard & Carter 1968; Parrish *et al.* 1976; Kronenberg & Tullis 1984; Koch *et al.* 1989). We have used the most recent experimental calibrations carried out by Luan & Paterson (1992) in the gas-apparatus and by Gleason & Tullis (1995) in the molten salt cell-technique in the Griggs-type piston-cylinder apparatus since the mechanical data of their studies are quite well constrained. Additionally, the geologically constrained, 'theoretical' flow laws of Paterson & Luan (1990) and Hirth *et al.* (2001) are considered in this study. The necessary coefficients for the flow laws are listed in Table 2.

In Fig. 7a the lines of constant strain rates corresponding to the flow laws of Luan & Paterson (1992) and Gleason & Tullis (1995; Table 2) as well as to the geologically constrained flow law of Paterson & Luan (1990) are compared with the data from this study. The comparison yields an estimate of the strain rate in the range of 10^{-14} to 10^{-12} s $^{-1}$ (Fig. 7a). This estimate is within the traditionally inferred range for natural fault zone conditions (e.g. Pfiffner & Ramsay 1982; Suppe 1985; Twiss & Moores 1992). The two orders of magnitude difference in the estimated strain rate (Fig. 7a) is due to the different flow law coefficients, which are partly caused by experimental differences in water fugacity. For H $_2$ O-saturated quartz aggregates the confining pressure is equal to the H $_2$ O-pressure (for both the Tonale fault zone samples and the experiments of Luan & Paterson 1992 it is about 300 MPa). The experiments of Gleason & Tullis (1995)

Table 2. Quartz flow law coefficients of flow laws used in this study

	Q [kJ mol ⁻¹]	A [MPa ⁻ⁿ s ⁻¹]	n
Luan & Paterson (1992)	152	4×10^{-10}	4
Gleason & Tullis (1995)	223	1.1×10^{-4}	4
Paterson & Luan (1990)	135	6.5×10^{-8}	3.1
Hirth <i>et al.</i> (2001)	135	6.30957×10^{-12}	4

Experimental calibrations from Luan & Paterson (1992) and Gleason & Tullis (1995); coefficients presented by Paterson & Luan (1990) and Hirth *et al.* (2001) are constrained by quartzite rheology and microstructural comparison.

were carried out at 1.5 GPa confining pressure with 0.15 weight% of added water. Kohlstedt *et al.* (1995) introduced a water fugacity term into the flow law equation:

$$\dot{\epsilon} = A \Delta\sigma^{-n} (f_{\text{H}_2\text{O}})^m \exp(-Q/RT), \quad (2)$$

where $\dot{\epsilon}$ is the strain rate, $\Delta\sigma$ is the differential stress, T is the temperature, R is the Boltzmann constant per mole, Q is the creep activation energy per mole, $f_{\text{H}_2\text{O}}$ is the water fugacity, A is a material constant, n is the stress exponent and m the water fugacity exponent. Saturated water conditions are a reasonable assumption for the samples of the eastern Tonale Fault Zone because of the H₂O-releasing metamorphic reactions in the metasediments of the shear zone, the quite homogeneous microstructures of dynamic recrystallization (local changes in water content may cause a switch in the dominant deformation mechanism and may thus produce a different

microstructure) and the abundance of fluid inclusions in the porphyroclasts.

In order to reduce differences in water fugacity the flow laws of Gleason & Tullis (1995) and Hirth *et al.* (2001) were normalized to the water fugacity at a pressure of 300 MPa, i.e. the confining pressure of the Tonale mylonites and the experiments of Luan & Paterson (1992), using a fugacity exponent of $m = 1$ (cf. Kohlstedt *et al.* 1995; Hirth *et al.* 2001). For the flow law of Gleason & Tullis (1995) the water fugacity coefficients after Tödheide (1972) were extrapolated to a confining pressure of 1.5 GPa (Fig. 7b). All flow laws indicate that the strain rate increases somewhat towards higher temperatures for the Tonale mylonites (using the stresses indicated by the Twiss-paleopiezometer relation). The strain rates, however, show considerable difference between the flow laws (Fig. 7b). Kohlstedt *et al.* (1995) come to a similar conclusion.

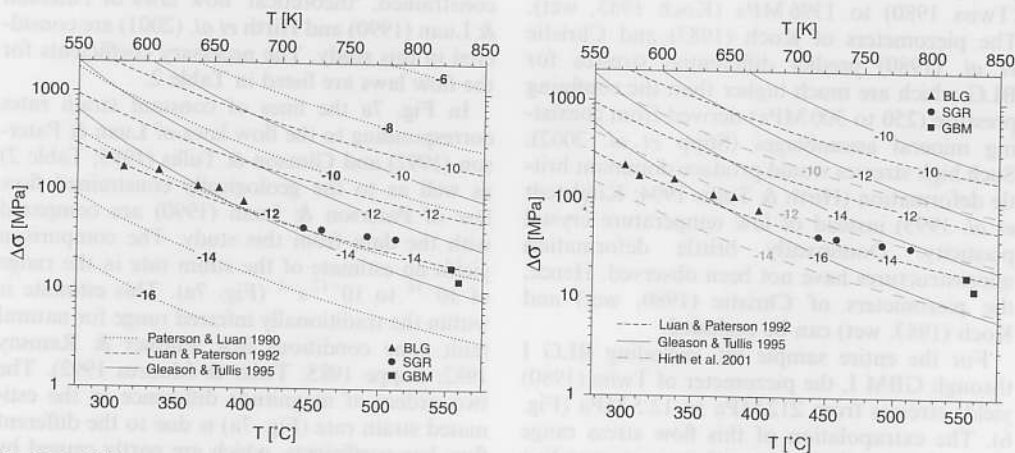


Fig. 7. (a) Flow stress data of the Tonale line samples (using the piezometer of Twiss 1980) plotted versus deformation temperature. Curves of constant strain rate are calculated from the flow laws of Luan & Paterson (1992), Gleason & Tullis (1995) and Paterson & Luan (1990). No account is taken of water fugacity differences. (b) Flow stress data of the Tonale line samples (using the piezometer of Twiss 1980) plotted versus deformation temperature. The curves of constant strain rate from the flow laws of Gleason & Tullis (1995) and Hirth *et al.* (2001) are normalized to a water fugacity at a confining pressure of 300 MPa and a fugacity exponent $m = 1$ so that all data sets have equivalent water fugacity conditions.

Their extrapolation of the laboratory data of Gleason & Tullis (1995) and Luan and Paterson (1992) to crustal deformation conditions at a constant strain rate leads to substantial differences in the predicted rock strength between the two data sets.

Discussion

Natural constraints on deformation along the Tonale Fault Zone

In the larger scale geological framework, the Tonale Line is a predominantly cataclastic fault zone (Schmid *et al.* 1989), which was active over at least 15 Ma (Müller 1998) with a dextral displacement of approximately 100 km (Laubscher 1991; Steck & Hunziker 1994; Frisch *et al.* 1998; Schmid & Kissling 2000) and a mean width of the fault zone of approximately 200 m. Hence, a reasonably fast shear strain rate estimate of approximately 10^{-12} s^{-1} results for this fault zone. Within that fault system, the investigated local Southern Mylonite Zone has formed as a consequence of a small local heat anomaly caused by the Adamello intrusion (Werling 1992). Thus, the deformation of the investigated mylonites is controlled by the larger kinematic framework of the entire Tonale fault zone and it can be inferred that the local mylonite strain rate results from the external kinematic boundary conditions related to plate movements. The actual local shear strain rate of the mylonites may vary from the overall estimate because of strain partitioning, variable shear zone width etc. The externally imposed shear strain rate of approximately 10^{-12} s^{-1} agrees best with the strain rate derived from the geologically constrained flow law of Hirth *et al.* (2001; Fig. 7b). Strain rates of 10^{-15} s^{-1} and slower are derived from the flow law of Gleason and Tullis (1995; Fig. 7b). Such slow strain rates are not in the range of typical geological strain rates (e.g. Pfiffner & Ramsay 1982) and are probably too low for the Tonale Line (see above).

Recrystallized grain size

Grain size reduction during dynamic recrystallization is observed in the case of BLG and SGR microstructures. As pointed out by Schmid and Handy (1991) syntectonic grain boundary migration recrystallization may lead to a decrease or an increase in size of the recrystallized grains. The very large grains in the GBM II zone, close to

the magmatic contact, may indicate such a grain size increase. The recrystallized grain sizes may have been modified after deformation ceased, either by annealing or by deformation at decreasing temperatures. Lower temperature overprints have been excluded, since only samples in which the microstructure could clearly be related to the synkinematic mineral assemblages used for the temperature estimates (cf. Stipp *et al.* 2002) have been selected. Microstructural features indicative of annealing, e.g. straight grain boundaries and increased grain sizes, are rare and only occur in the GBM II zone. The fact that subgrains and recrystallized grains in the zone of SGR (observed in the light microscope) have identical sizes is further evidence that postdeformational grain growth is not important. Therefore, corrections for grain growth (Hacker *et al.* 1990, 1992) are not necessary for the investigated sample set. Microstructural evidence for posttectonic grain growth in the Tonale mylonites is absent and indicates that posttectonic grain growth had only a minor effect because of the relatively rapid cooling after contact metamorphism. Fast cooling was caused by: (1) the low depth (approximately 8 km) of mylonitization of the investigated section; and (2) because colder rocks were continuously passing along the intrusion during the strike-slip movement of the fault zone (advective cooling). The rapid cooling is confirmed by the small difference between U/Pb-ages on zircon ($32.0 \pm 2.3 \text{ Ma}$; Stipp 2001) Rb/Sr-ages on muscovite ($31.3 \pm 1.5 \text{ Ma}$; Del Moro *et al.* 1983) and K/Ar and Rb/Sr ages on muscovite ($\sim 29.5 \pm 2 \text{ Ma}$; Del Moro *et al.* 1983) of the Presanella granitoids in the Adamello pluton, indicating fast cooling of the magmatic body.

Evaluation of paleopiezometers

The different slopes of the flow-stress versus temperature curves calculated for different recrystallization mechanisms (Fig. 6) indicate that, ideally, piezometers should be adjusted for different recrystallization mechanisms. The need to define different piezometers for different recrystallization mechanisms was first stated by Poirier and Guillopé (1979) and experimentally calibrated for halite (SGR, GBM) by Guillopé and Poirier (1979). A number of piezometers, which depend on the dynamic recrystallization mechanism, have been proposed for other rock-forming minerals, e.g. for calcite (SGR, GBM; Schmid *et al.* 1980; Rutter 1995), olivine (GBM; van der Wal *et al.* 1993). Post and Tullis (1999) showed that the slope of the

stress–grain size relationship for the regime 1 piezometer of feldspar varies from that for regime 2 for other minerals. In the case of quartz, however, none of the proposed piezometers takes the recrystallization mechanism into account (cf. White 1982). Only the piezometer of Twiss (1977, 1980) is in quite good agreement with the most recent experimental studies on crystal plastic deformation of quartz aggregates (Gleason & Tullis 1993). Gleason and Tullis (1995) and Hirth *et al.* (2001) find the piezometer of Twiss (1977) the most accurate for the transition between regime 2 and 3 and for regime 3, and they recommend the use of this relationship for SGR and at the SGR/GBM transition until new experimental calibrations are available. This study also finds that the relation of Twiss (1977, 1980) is the most consistent paleopiezometer for geological deformation conditions within the zone of BLG. We are aware of the fact that the piezometer of Twiss (1977) is based on questionable assumptions of equilibrium thermodynamics, as pointed out in Poirier (1985), Derby (1990) and de Bresser *et al.* (2001). Yet we recommend its application because of its best fit to currently published experimental and natural data on the dynamic recrystallization of quartz.

The comparison between subgrains and recrystallized grains in the Tonale mylonites (observed in the light microscope) does not show a significant difference in size. However, subgrains can only be measured grain by grain and such measurements have not been included in this study because a profound statistical base is lacking. Furthermore, the difference between the larger subgrains determined in the light microscope compared to those determined in the TEM is not yet understood. Nevertheless, if we assume that the light optically determined subgrains represent the precursors towards progressive rotation and recrystallization without a significant variation in size, the same stress dependency for subgrains and recrystallized grains could apply (Schmid *et al.* 1980). In that case, the temperature seems not to have a major influence on the recrystallized grain size during ongoing recrystallization. Equal diameters of bulges and recrystallized grains in the samples also suggest the absence of thermally induced grain growth during and after dynamic recrystallization for the zone of BLG. The absence of thermally induced grain growth is in agreement with the considerations of Post and Tullis (1999) who point out that migration rate and strain rate have the same temperature dependence and, thus, the resulting recrystallized grain size is not temperature dependent. In addition, in

experiments on Carrara marble, Rutter (1995) does not find a significant influence of temperature and strain rate on the recrystallized grain size. Instead, the same author finds a clear stress dependence and a difference between the piezometer for subgrain rotation recrystallization and that for grain boundary migration recrystallization. Hence, there is, so far, no experimental evidence for an important temperature effect on the dynamically recrystallized grain size of major rheologically relevant minerals. This is despite the theoretical models of Derby & Ashby (1987), Derby (1990), Shimizu (1998) and de Bresser *et al.* (1998), all of which include a (weak) temperature dependency via the activation energy term. Our results indicate that well constrained experimental data on quartz in terms of physical parameters (T , $\Delta\sigma$, ϵ , $\dot{\epsilon}$, f_{H_2O}), recrystallized grain and subgrain size, and steady state recrystallization microstructures, will be required, before we can evaluate microphysical models of piezometers for quartz, as presented and discussed in de Bresser *et al.* (2001).

A deformation mechanism map of dynamic recrystallization

Hirth and Tullis (1992) plotted the results of their experiments on a strain rate versus temperature diagram. This type of diagram has also been proposed by Frost and Ashby (1982) as one possible presentation of deformation mechanism maps. The presentation of dynamic recrystallization mechanisms in a strain rate versus temperature plot has several advantages: (1) the extrapolation of deformation experiments to natural conditions is an extrapolation in strain rate; and (2) as pointed out by Handy (1989), time and strain can sometimes be derived directly from geological observations and isotopic studies so that in certain cases the natural strain rate can be determined independent of experimental flow laws.

The data set from the Tonale fault zone is plotted in such a strain rate versus temperature diagram (Fig. 8) together with the experimental data of Hirth and Tullis (1992) and another natural sample set from the Ruby Gap Duplex in Central Australia (Dunlap *et al.* 1997). The strain rates of the natural samples were calculated using flow laws, as discussed above (Fig. 8a). The two natural sample sets (Dunlap *et al.* 1997 and the Tonale mylonites) cover a range of strain rates from 10^{-20} to 10^{-11} s $^{-1}$. Strain rates of 10^{-20} to 10^{-15} s $^{-1}$ appear unrealistically slow, because strain rates of 10^{-15} s $^{-1}$ and

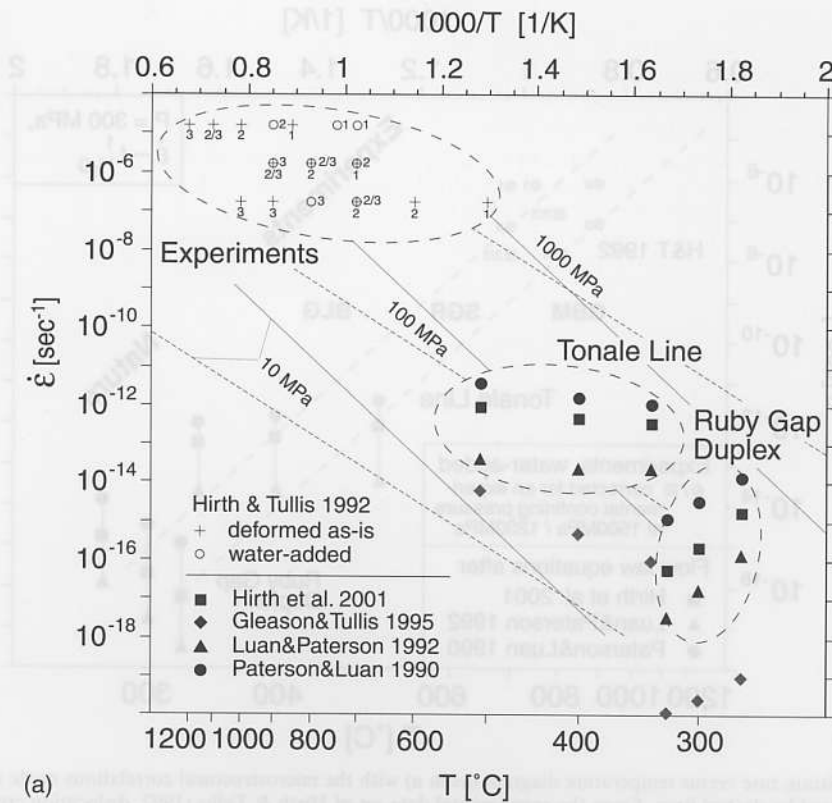


Fig. 8. (a) Strain rate versus temperature diagram showing the experimental data of Hirth & Tullis (1992), natural samples from the Tonale Line (this study) and those of the Ruby Gap Duplex (Dunlap *et al.* 1997). Only microstructures at transitions BLG I – BLG II (sample 26-2), BLG II – SGR (sample 24-4) and SGR – GBM I (sample 15-2) are used; data from Dunlap *et al.* (1997) have been reinterpreted using microstructural criteria discussed here. Deformation temperatures are taken from Dunlap *et al.* (1997) and Stipp *et al.* (subm.), and the flow stress data required for flow law calculations were derived from the piezometer of Twiss (1977; 1980). The natural strain rates have been calculated from four different flow laws. Experiments of Hirth & Tullis (1992) were carried out 'as-is' (crosses) or with added water (open circles); the dislocation creep regimes are indicated by the numbers. Lines of constant flow stress from the flow laws of Luan & Paterson (1992, dashed lines) and Gleason & Tullis (1995, solid lines) are displayed.

slower are not believed to leave microstructural traces in the rock (Pfiffner & Ramsay 1982). Thus, strain rates derived from the experimental flow laws of Gleason & Tullis (1995) and Luan & Paterson (1992) produce unrealistic results for the two natural sample sets. The geologically constrained empirical flow laws of Paterson & Luan (1990) and Hirth *et al.* (2001) show a strain rate of approximately 10^{-12} s^{-1} which is consistent with other geological constraints for the Tonale Line. The faster strain rates for the Ruby Gap samples of approximately 10^{-15} s^{-1} to 10^{-14} s^{-1} predicted by Paterson & Luan (1992) and Hirth *et al.* (2001) are also in the range of natural rock deformation. From the study of Hirth and Tullis (1992), both 'as-is' and water-added experiments are plotted (Fig.

8a). Together with the naturally deformed samples of the Ruby Gap Duplex (Dunlap *et al.* 1997) and the Tonale samples, there are now three data sets available to define the transitions of recrystallization mechanisms in a strain rate versus temperature diagram (Fig. 8a, b). Straight lines in a log strain rate versus $1/T$ plot imply constant stress conditions (Hirth *et al.* 2001). As a consequence of constant stress conditions, the grain sizes along the transitions should be constant. However, the recrystallized grain size in the experimental samples is much smaller than in the Tonale samples for corresponding recrystallization mechanisms (compare the experimentally and naturally deformed samples in Fig. 3). Thus, it remains questionable that the transitions between different recrystallization

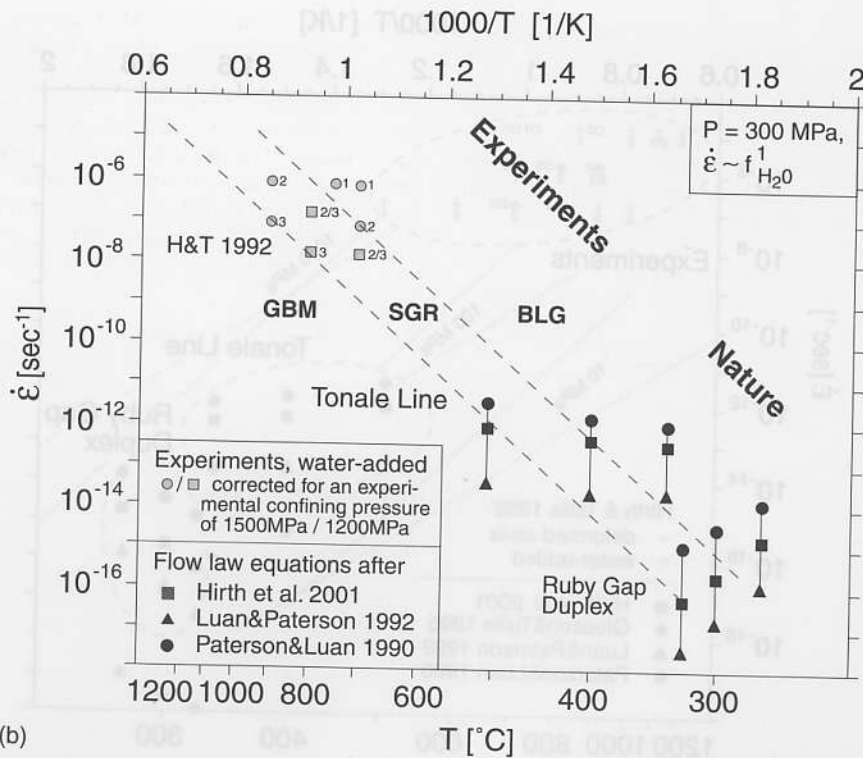


Fig. 8. (b) Strain rate versus temperature diagram (as in a) with the microstructural correlations made in this study indicated by dashed lines. From the experimental data set of Hirth & Tullis (1992, dislocation creep regimes are indicated by the numbers) only the water-added samples are used. Water fugacity is normalized to a confining pressure of 300 MPa.

mechanisms correspond to constant stress curves for a given flow law. The great temperature difference between corresponding natural and experimental recrystallization mechanisms might also effect a difference in the recrystallized grain size as discussed by de Bresser *et al.* (1998, 2001). At present, however, there is no experimental proof for this difference in quartz, as pointed out above.

Several adjustments must be made for correlating experimental and natural sample sets. The experiments of Hirth and Tullis (1992) were carried out in a solid medium apparatus, and the derived flow stresses tend to be overestimated. Water has pronounced weakening effects at high confining pressures and a correction needs to be applied to extrapolate flow stresses to lower pressures. One procedure for such a correction is to introduce the water fugacity with an exponent m as a coefficient into the flow law, as has been described before (cf. Kohlstedt *et al.* 1995; Post *et al.* 1996; Hirth *et al.* 2001). Thus, the experimental data points in Fig. 8a are shifted to slower strain rates (or

higher temperatures) if normalized to the confining pressures of the naturally deformed samples at 300 MPa. The iso-stress lines of the Luan and Paterson (1992) flow law (dashed lines) and of the Gleason and Tullis (1995) flow law (solid lines) for uncorrected experimental data points are added for comparison.

The microstructural similarities between all sample sets are striking, so that it appears safe to correlate the natural and experimental conditions of temperature and strain rate for dynamic recrystallization. It is suggested that natural and experimental transitions of dynamic recrystallization mechanisms may follow a straight curve fit in a logarithmic strain rate versus $1/T$ plot. Such a fit of the boundaries between the three recrystallization mechanisms is indicated by the two dashed lines in Fig. 8b. Only the water-added samples have been used from the data set. These experiments have been carried out in NaCl- and pyrophyllite-cells (Jan Tullis, pers. comm.). Johannes (1978) found that the effective confining pressure in NaCl-cell assemblies corresponds to the externally measured pressure

and that the effective confining pressure in pyrophyllite assemblages is about 20% lower than in NaCl-assemblages. Based on his findings we recalculated strain rates for the Hirth & Tullis (1992) data set with a water fugacity for an effective confining pressure of 1.5 GPa and 1.2 GPa for the salt and the pyrophyllite assemblages, respectively (Fig. 8b).

The diagram shows that the recrystallization mechanism transitions primarily depend on temperature and strain rate. Changing one of these two variables will change the dominant dynamic recrystallization mechanism. According to the reported predominance of relative constant natural strain rate conditions on the order of 10^{-14} to 10^{-12} s^{-1} (e.g. Mercier *et al.* 1977; Pfiffner & Ramsay 1982; Suppe 1985; Twiss & Moores 1992) microstructural changes have usually been related to temperature changes as is obvious for e.g. the Tonale mylonites or the Ruby Gap Duplex (Dunlap *et al.* 1997). However, major changes in the strain rate and related flow stress conditions at relatively small temperature variations have also been observed in conjunction with changes in the dominant recrystallization microstructure (e.g. White 1982; Stipp 2001). Because of the importance of dynamic recrystallization of quartz in mylonitic shear zones this recrystallization mechanism map is applicable to most natural deformation conditions. In contrast to the deformation mechanism maps previously constructed for quartz (e.g. Rutter 1976; White 1976; Etheridge and Wilkie 1979), which are largely based on theoretical assumptions and calculations, the recrystallization mechanism map in Fig. 8b is derived from experimental as well as natural data. The map includes the complete field of dislocation creep and covers the dynamic recrystallization microstructures of quartz occurring in natural mylonitic fault rocks. Additional experimental and geological field studies encompassing a broad spectrum of metamorphic conditions (e.g. Stöckhert *et al.* 1999; Zulauf 2001) are necessary to better constrain this dynamic recrystallization mechanism map.

We consider this study as an attempt to demonstrate that estimations of temperature and strain rate may be made by characterizing dynamic recrystallization microstructures. The geological application is fairly straightforward. The dynamic recrystallization mechanism (BLG, SGR, GBM) has to be determined from the microstructure of quartz (preferably in pure quartz aggregates). If the deformation temperature can be determined (e.g. from syndeformational mineral assemblages), then the range of strain rates can be determined from the recrystal-

lization mechanism map. Alternatively, if age data are available which allow for an estimate of the strain rate within a shear zone, the recrystallization mechanism map provides an independent tool for the determination of deformation temperatures. The recognition of the recrystallization mechanism is valuable because it may help to constrain deformation temperatures and strain rates within a usually narrow range of natural fault zone conditions in the upper crust.

Summary and conclusions

Dynamic recrystallization microstructures of quartz have been used as a link between nature and experiment. The recrystallization microstructures of the eastern Tonale mylonites have been correlated with the experimental dislocation creep regimes of Hirth & Tullis (1992). From the Tonale mylonites, temperature, stress and strain rate data can be determined, using the Twiss theoretical recrystallized grain size piezometer for all recrystallization mechanisms and quartzite flow laws adjusted for water fugacity. The data from naturally deformed quartz can help to constrain piezometers and flow laws. There is a need for quartz paleopiezometers to be calibrated for different recrystallization mechanisms. Natural and experimental data sets of dynamic recrystallization microstructures and dislocation creep regimes can be plotted on a strain rate versus temperature diagram. The fields of the different recrystallization microstructures are separated by transition zones, and their trend is consistent in nature and experiment. Using microstructural correlations, a recrystallization mechanism map can be derived from this diagram. This map may be used for either estimating strain rates (if the temperature is known) or temperature (if the strain rate is known) from studying the recrystallization microstructure.

We are greatly indebted to J. Tullis and G. Hirth for their continued and enthusiastic support and their critical scrutiny toward this study. J. Tullis critically reviewed an early version of this paper and suggested a number of important improvements. The constructive reviews of J. L. Urai and J. C. White and the editorial comments of J. H. P. de Bresser and G. Pennock are gratefully acknowledged. This work is funded by the Swiss National Science Foundation (grants 20-49562.96 and 2000-055420.98).

References

- BAILEY, J. E. & HIRSCH, P. B. 1962. The recrystallization process in some polycrystalline metals. *Proceedings of the Royal Society of London*, **A267**, 11–30.

- CHRISTIE, J. M., ORD, A. & KOCH, P. S. 1980. Relationship between recrystallized grain size and flow stress in experimentally deformed quartzite. *EOS Transactions*, **61/17**, 377.
- DE BRESSER, J. H. P., PEACH, C. J., REIJS, J. P. J. & SPIERS, C. J. 1998. On dynamic recrystallization during solid state flow: effects of stress and temperatures. *Geophysical Research Letters*, **25**, 3457–3460.
- DE BRESSER, J. H. P., TER HEEGE, J. H. & SPIERS, C. H. 2001. Grain size reduction by dynamic recrystallization: can it result in major rheological weakening? *International Journal of Earth Sciences*, **90**, 28–45.
- DEL MORO, A., PARDINI, G., QUERCIOLO, C., VILLA, I. M. & CALLEGARI, E. 1983. Rb/Sr and K/Ar chronology of Adamello granitoids, Southern Alps. *Memorie della Società Geologica Italiana*, **26**, 285–299.
- DERBY, B. 1990. Dynamic recrystallization and grain size. In: BARBER, D. J. & MEREDITH, P. G. (eds) *Deformation Processes in Minerals, Ceramics and Rocks*. Unwin Hyman, London, 354–364.
- DERBY, B. & ASHBY, M. F. 1987. On dynamic recrystallization. *Scripta Metallurgica*, **21**, 879–884.
- DOHERTY, R. D., HUGHES, D. A. ET AL. 1997. Current issues in recrystallization: a review. *Materials Science and Engineering*, **A238**, 219–274.
- DRURY, M. R., HUMPHREYS, F. J. & WHITE, S. H. 1985. Large strain deformation studies using polycrystalline magnesium as a rock analogue. Part II: dynamic recrystallisation mechanisms at high temperatures. *Physics of the Earth and Planetary Interiors*, **40**, 208–222.
- DUNLAP, W. J., HIRTH, G. & TEYSSIER, C. 1997. Thermo-mechanical evolution of a ductile duplex. *Tectonics*, **16**, 983–1000.
- EDWARD, G. H., ETHERIDGE, M. A. & HOBBS, B. E. 1982. On the stress dependence of subgrain size. *Textures and Microstructures*, **5**, 127–152.
- ETHERIDGE, M. A. & WILKIE, J. C. 1979. Grain size reduction, grain boundary sliding and the flow strength of mylonites. *Tectonophysics*, **58**, 159–178.
- EVANS, B., FREDRICH, J. T. & WONG, T.-F. 1990. The brittle-ductile transition in rocks: recent experimental and theoretical progress. In: DUBA A. G., DURHAM, W. B., HANDIN, J. W. & WANG, H. F. (eds) *The Brittle-Ductile Transition in Rocks*. *Geophysical Monograph*, **56**, 1–20.
- FITZ GERALD, J. D. & STÜNITZ, H. 1993. Deformation of granitoids at low metamorphic grade. I: reactions and grain size reduction. *Tectonophysics*, **221**, 269–297.
- FRISCH, W., KUHLEMANN, J., DUNKL, I. & BRUGEL, A. 1998. Palinspastic reconstruction and topographic evolution of the eastern Alps during late Tertiary tectonic extrusion. *Tectonophysics*, **297**, 1–15.
- FROST, H. J. & ASHBY, A. F. 1982. *Deformation Mechanism Maps*. Pergamon Press, Oxford.
- GLEASON, G. C. & TULLIS, J. 1993. Improving flow laws and piezometers for quartz and feldspar aggregates. *Geophysical Research Letters*, **20**, 2111–2114.
- GLEASON, G. C. & TULLIS, J. 1995. A flow law for dislocation creep of quartz aggregates determined with the molten salt cell. *Tectonophysics*, **247**, 1–23.
- GOETZE, C. & KOHLSTEDT, D. L. 1973. Laboratory study of dislocation climb and diffusion in olivine. *Journal of Geophysical Research*, **78**, 5961–5971.
- GUILLOPÉ, M. & POIRIER, J. P. 1979. Dynamic recrystallization during creep of single-crystalline halite: an experimental study. *Journal of Geophysical Research*, **84**, 5557–5567.
- HACKER, B. R., YIN, A., CHRISTIE, J. M. & DAVIS, G. A. 1992. Stress magnitude, strain rate, and rheology of extended middle continental crust inferred from quartz grain sizes in the Whipple Mountains, California. *Tectonics*, **11**, 36–46.
- HACKER, B. R., YIN, A., CHRISTIE, J. M. & SNOKE, A. W. 1990. Differential stress, strain rate, and temperatures of mylonitization in the Ruby Mountains, Nevada: implications for the rate and duration of uplift. *Journal of Geophysical Research*, **95**, 8569–8580.
- HANDY, M. R. 1989. Deformation regimes and the rheological evolution of fault zones in the lithosphere: the effects of pressure, temperature, grain size and time. *Tectonophysics*, **163**, 119–152.
- HEARD, H. C. & CARTER, N. L. 1968. Experimentally induced 'natural' intragranular flow in quartz and quartzite. *American Journal of Science*, **266**, 1–42.
- HIPPERT, J. & EGYDIO-SILVA, M. 1996. New polygonal grains formed by dissolution-redeposition in quartz mylonite. *Journal of Structural Geology*, **18**, 1345–1352.
- HIRTH, G. & TULLIS, J. 1992. Dislocation creep regimes in quartz aggregates. *Journal of Structural Geology*, **14**, 145–159.
- HIRTH, G. & TULLIS, J. 1994. The brittle-plastic transition in experimentally deformed quartz aggregates. *Journal of Geophysical Research*, **99**, 11731–11747.
- HIRTH, G., TEYSSIER, C. & DUNLAP, W. J. 2001. An evaluation of quartzite flow laws based on comparisons between experimentally and naturally deformed rocks. *International Journal of Earth Sciences*, **90**, 77–87.
- HOBBS, B. E. 1968. Recrystallization of single crystals of quartz. *Tectonophysics*, **6**, 353–401.
- HOBBS, B. E., MEANS, W. D. & WILLIAMS, P. F. 1976. *An Outline of Structural Geology*. John Wiley & Sons, New York.
- HUMPHREYS, F. J. & HATHERLY, M. 1996. *Recrystallization and Related Annealing Phenomena*. Pergamon Press, Oxford.
- JESSELL, M. W. 1987. Grain-boundary migration microstructures in a naturally deformed quartzite. *Journal of Structural Geology*, **9**, 1007–1014.
- JOHANNES, W. 1978. Pressure comparing experiments with NaCl, AgCl, talc, and pyrophyllite assemblies in a piston cylinder apparatus. *Neues Jahrbuch Mineralogische Monatshefte*, **2**, 84–92.
- KIRBY, S. H. 1980. Tectonic stresses in the lithosphere: Constraints provided by the experimental deformation of rocks. *Journal of Geophysical Research*, **85**, 6353–6363.

- KOCH, P. S. 1983. *Rheology and Microstructures of Experimentally Deformed Quartz Aggregates*. PhD thesis, University of California.
- KOCH, P. S., CHRISTIE, J. M., ORD, A. & GEORGE, R. P. 1989. Effect of water on the rheology of experimentally deformed quartzite. *Journal of Geophysical Research*, **94**, 13975–13996.
- KOHLSTEDT, D. L. & WEATHERS, M. S. 1980. Deformation induced microstructures, paleopiezometers and differential stresses in deeply eroded fault zones. *Journal of Geophysical Research*, **85**, 6269–6285.
- KOHLSTEDT, D. L., EVANS, B. & MACKWELL, S. J. 1995. Strength of the lithosphere: constraints imposed by laboratory experiments. *Journal of Geophysical Research*, **100**, 17587–17602.
- KRONENBERG, A. & TULLIS, J. 1984. Flow strengths of quartz aggregates: grain size and pressure effects due to hydrolytic weakening. *Journal of Geophysical Research*, **89**, 4281–4297.
- KÜSTER, M. & STRÖCKHERT, B. 1999. High differential stress and sublithostatic pore fluid pressure in the ductile regime – microstructural evidence for short-term post-seismic creep in the Sesia Zone, Western Alps. *Tectonophysics*, **303**, 263–277.
- LAUBSCHER, H. 1991. The arc of the Western Alps today. *Eclogae geologicae Helvetiae*, **84**, 631–659.
- LUAN, F. C. & PATERSON, M. S. 1992. Preparation and deformation of synthetic aggregates of quartz. *Journal of Geophysical Research*, **97**, 301–320.
- LUTON, M. J. & SELLARS, C. M. 1969. Dynamic recrystallization in nickel and nickel-iron alloys during high temperature deformation. *Acta Metallurgica*, **17**, 1033–1043.
- MAINPRICE, D. H. 1981. *The Experimental Deformation of Quartz Polycrystals*. PhD thesis, Australian National University.
- MCQUEEN, H. J., KNUSTAD, O., RYUM, N. & SOLBERG, J. K. 1985. Microstructural evolution in Al deformed to strains of 60 at 400 °C. *Scripta Metallurgica*, **19**, 73–78.
- MEANS, W. D. 1983. Microstructure and micro-motion in recrystallization flow of Octachloropropane: a first look. *Geologische Rundschau*, **72**, 511–528.
- MERCIER, J.-C. C. 1980. Magnitude of continental lithospheric stress inferred from rheomorphic petrology. *Journal of Geophysical Research*, **85**, 6293–6303.
- MERCIER, J.-C. C., ANDERSON, D. A. & CARTER, N. L. 1977. Stress in the lithosphere: inferences from steady state flow of rocks. *Pure and Applied Geophysics*, **115**, 199–226.
- MÜLLER, W. 1998. *Isotopic Dating of Deformation Using Microsampling Techniques: The Evolution of the Periadriatic Fault System (Alps)*. PhD thesis, ETH Zürich.
- ORD, A. & CHRISTIE, J. M. 1984. Flow stresses from microstructures in mylonitic quartzites of the Moine Thrust zone, Assynt area, Scotland. *Journal of Structural Geology*, **6**, 639–654.
- PANOZZO HEILBRONNER, R. 1992. The autocorrelation function: an image processing tool for fabric analysis. *Tectonophysics*, **212**, 351–370.
- PANOZZO HEILBRONNER, R. & PAULI, C. 1993. Integrated spatial and orientation analysis of quartz c-axes by computer-aided microscopy. *Journal of Structural Geology*, **15**, 369–382.
- PANOZZO HEILBRONNER, R. & PAULI, C. 1994. Orientation and misorientation imaging: integration of microstructural and textural analysis. In: BUNGE, H. J., SIEGSMUND, S., SKROTZKI, W. & WEBER, K. (eds) *Textures of Geological Materials*. DGM Informationsgesellschaft Verlag, Oberursel, 147–164.
- PARRISH, D. K., KRIVZ, A. L. & CARTER, N. L. 1976. Finite-element folds of similar geometry. *Tectonophysics*, **32**, 183–207.
- PATERSON, M. S. 1987. Problems in the extrapolation of laboratory rheological data. *Tectonophysics*, **133**, 33–43.
- PATERSON, M. S. & LUAN, F. C. 1990. Quartzite rheology under geological conditions. In: KNIPE, R. J. & RUTTER, E. H. (eds) *Deformation mechanisms, rheology and tectonics*. Geological Society, London, Special Publication, **54**, 299–307.
- PIFFNER, O. A. & RAMSAY, J. G. 1982. Constraints on geological strain rates: arguments from finite-strain states of naturally deformed rocks. *Journal of Geophysical Research*, **87**, 311–321.
- POIRIER, J.-P. 1985. *Creep of Crystals*. Cambridge University Press, Cambridge.
- POIRIER, J. P. & GUILLOPÉ, M. 1979. Deformation-induced recrystallization of minerals. *Bulletin de la Société française de Minéralogie et de Cristallographie*, **102**, 67–74.
- POST, A. & TULLIS, J. 1999. A recrystallized grain size paleopiezometer for experimentally deformed feldspar aggregates. *Tectonophysics*, **303**, 159–173.
- POST, A. D., TULLIS, J. & YUND, A. 1996. Effects of chemical environment on dislocation creep of quartzite. *Journal of Geophysical Research*, **101**, 22143–22155.
- RALEIGH, C. B. & KIRBY, S. H. 1970. Creep in the upper mantle. *Mineralogical Society of America Special Paper*, **3**, 113–121.
- RANALLI, G. 1984. Grain size distribution and flow stress in tectonites. *Journal of Structural Geology*, **6**, 443–447.
- RASBAND, W. 1996. *NIH Image*. National Institute of Health, Research Services Branch NIMH.
- RUTTER, E. H. 1976. The kinetics of rock deformation by pressure solution. *Philosophical Transactions of the Royal Society of London*, **A283**, 203–219.
- RUTTER, E. H. 1995. Experimental study of the influence of stress, temperature, and strain on the dynamic recrystallization of Carrara marble. *Journal of Geophysical Research*, **100**, 24651–24663.
- SCHMID, S. M. & HANDY, M. R. 1991. Towards a genetic classification of fault rocks: geological usage and tectonophysical implications. In: MÜLLER, D. W., MCKENZIE, J. A. & WEISSERT, H. (eds) *Controversies in Modern Geology*. Academic Press, London, 339–361.
- SCHMID, S. M. & KISSLING, E. 2000. The arc of the Western Alps in the light of new data on deep crustal structure. *Tectonics*, **19**, 62–85.

- SCHMID, S., AEBLI, H. R., HELLER, F. & ZINGG, A. 1989. The role of the Periadriatic Line in the tectonic evolution of the Alps. In: COWARD, M. P., DIETRICH, D. & PARK, R. G. (eds) *Alpine Tectonics*. Geological Society, London, Special Publications, **45**, 153–171.
- SCHMID, S. M., PATERSON, M. S. & BOLAND, J. N. 1980. High temperature flow and dynamic recrystallization in Carrara marble. *Tectonophysics*, **65**, 245–280.
- SHIMIZU, I. 1998. Stress and temperature dependence of recrystallized grain size: a subgrain misorientation model. *Geophysical Research Letters*, **25**, 4237–4240.
- SMITH, C. S. & GUTTMAN, L. 1953. Measurement of internal boundaries in the three-dimensional structures by random sectioning. *Transactions of the American Institute of Mining and Metallurgical Engineers, Journal of Metals*, **197**, 81–87.
- SNOKE, A. W., TULLIS, J. & TODD, V. R. (eds.) 1998. *Fault-Related Rocks*. Princeton University Press, Princeton.
- STECK, A. & HUNZIKER, J. 1994. The Tertiary structural and thermal evolution of the Central Alps – compressional and extensional structures in an orogenic belt. *Tectonophysics*, **238**, 229–254.
- STIPP, M. 2001. *Dynamic Recrystallization of Quartz in Fault Rocks from the Eastern Tonale Line (Italian Alps)*. PhD thesis, University of Basel.
- STIPP, M. & SCHMID, S. M. 1998. Evidence for the contemporaneity of movements along the Tonale line and the intrusion of parts of the Adamello batholith. *Memorie di Scienze Geologiche*, **50**, 89–90.
- STIPP, M., STÜNITZ, H., HEILBRONNER, R. AND SCHMID, S. M. 2002. The eastern Tonale fault zone: a 'natural laboratory' for crystal plastic deformation of quartz over a temperature range from 250 °C to 700 °C. *Journal of Structural Geology*, **24**, 1861–1884.
- STÖCKHERT, B., BRIX, M. R., KLEINSCHRODT, R., HURFORD, A. J. & WIRTH, R. 1999. Thermochronometry and microstructures of quartz – a comparison with experimental flow laws and predictions on the temperature of the brittle-plastic transition. *Journal of Structural Geology*, **21**, 351–369.
- SUPPE, J. 1985. *Principles of Structural Geology*. Prentice-Hall, Englewood Cliffs, New Jersey.
- TAKEUCHI, S. & ARGON, A. S. 1976. Steady state creep of single-phase-crystalline matter at high temperatures. *Journal of Materials Science*, **11**, 1542–1566.
- TÖDHEIDE, K. 1972. Water at high temperatures and pressures. In: FRANKS, F. (ed) *Water – A Comprehensive Treatise*, **1**, Plenum Press, New York, 463–514.
- TULLIS, J., STÜNITZ, H., TEYSSIER, C. & HEILBRONNER, R. 2000. Deformation microstructures in quartzofeldspathic rocks. In: JESSEL, M. W. & URAI, J. L. (eds) *Stress, Strain and Structure, a Volume in Honor of W D Means*. *Journal of the Virtual Explorer 2*. World Wide Web Address: http://www.virtualexplorer.com.au/VEjournal/2000Volumes/Volume2/www/contribs/tullis/SlideSet/deformation_micro.html
- TWISS, R. J. 1977. Theory and applicability of a recrystallized grain size paleopiezometer. *Pure and Applied Geophysics*, **115**, 227–244.
- TWISS, R. J. 1980. Static theory of size variation with stress for subgrains and dynamically recrystallized grains. In: USGS (ed) *Proceedings of the IX. Conference, Magnitude of Deviatoric Stresses in the Earth's Crust and Upper Mantle. Open File Report*, **80–625**, Menlo Park, California, 665–683.
- TWISS, R. J. 1986. Variable sensitivity piezometric equations for dislocation density and subgrain diameter and their relevance to olivine and quartz. In: HOBBS, B. E. & HEARD, H. C. (eds) *Mineral and Rock Deformation: Laboratory Studies*. Geophysical Monograph, **36**, 247–261.
- TWISS, R. J. & MOORES, E. M. 1992. *Structural Geology*. W. H. Freeman and Company, New York.
- URAI, J. L., MEANS, W. D. & LISTER, G. S. 1986. Dynamic recrystallization of minerals. In: HOBBS, B. E. & HEARD, H. C. (eds) *Mineral and Rock Deformation: Laboratory Studies*. Geophysical Monograph, **36**, 161–199.
- VAN DAALLEN, M., HEILBRONNER, R. & KUNZE, K. 1999. Orientation analysis of localized shear deformation in quartz fibres at the brittle-ductile transition. *Tectonophysics*, **303**, 83–107.
- VAN DER WAL, D., CHOPRA, P., DRURY, M. & FITZGERALD, J. 1993. Relationship between dynamically recrystallized grain size and deformation conditions in experimentally deformed olivine rocks. *Geophysical Research Letters*, **20**, 1479–1482.
- WEERTMAN, J. 1970. The creep strength of the Earth's mantle. *Reviews of Geophysics and Space Physics*, **8**, 145–168.
- WERLING, E. 1992. *Tonale-, Pejo- und Judicarien-Linie: Kinematik, Mikrostrukturen und Metamorphose von Tektoniten aus räumlich interferierenden aber verschiedenartigen Verwerfungszonen*. PhD thesis, ETH Zürich.
- WHITE, J. C. 1982. Quartz deformation and the recognition of recrystallization regimes in the Flinton Group conglomerates, Ontario. *Canadian Journal of Earth Sciences*, **19**, 81–93.
- WHITE, S. 1979. Grain and sub-grain size variations across a mylonite zone. *Contributions to Mineralogy and Petrology*, **70**, 193–202.
- WHITE, S. H. 1973. Syntectonic recrystallisation and texture development in quartz. *Nature*, **244**, 276–277.
- WHITE, S. H. 1976. The effects of strain on the microstructures, fabrics and deformation mechanisms in quartz. *Philosophical Transactions of the Royal Society of London*, **A283**, 69–86.
- ZULAUF, G. 2001. Structural style, deformation mechanisms and paleodifferential stress along an exposed crustal section; constraints on the rheology of quartzofeldspathic rocks at supra- and infrastructural levels (Bohemian Massif). *Tectonophysics*, **332**, 211–237.